Direct Detection of the Hybridization of Synthetic Homo-Oligomer DNA Sequences by Field Effect

E. Souteyrand,[†] J. P. Cloarec,[†] J. R. Martin,[†] C. Wilson,[‡] I. Lawrence,[‡] S. Mikkelsen,[‡] and M. F. Lawrence*[,‡]

Laboratoire de PhysicoChimie des Interfaces, Ecole Centrale de Lyon, BP 163, 69131 Ecully Cedex, France, and Department of Chemistry and Biochemistry, Concordia University, 1455 de Maisonneuve West, Montreal, Quebec, Canada H3G 1M8

Received: October 4, 1996; In Final Form: December 16, 1996[⊗]

Homo-oligomer DNA strands were immobilized onto silicon/silicon dioxide electrodes using 3-aminopropyltriethoxysilane. These modified substrates were used as working electrodes in a three-electrode electrochemical cell. In-phase and out-of-phase impedances were measured in the range −1 to +1 V with respect to an Ag/AgCl reference electrode, with a superimposed 10 mV ac signal at frequencies of 20 and 100 kHz. *Ex situ* hybridization with complementary oligomer strands, performed at the surface of modified electrodes, is clearly reflected by negative shifts of about 100 mV in the flat-band potential of the semiconductor. Consecutive hybridization−denaturation steps show that the shifts are reproducible and the process is reversible. The *in situ* hybridization of complementary strands has also been observed with impedance measurements at Si/SiO_2 substrates and with the use of a field effect device. The direct detection of hybridization with a field effect device was performed under constant drain current mode, and the corresponding variations observed for the gate potential during hybridization are in good agreement with the flat band potential shifts observed with the impedance experiments. Measurements made in the presence of noncomplementary strands demonstrate the selectivity of the device.

Introduction

Biotechnology and medical diagnostics are currently in need of devices able to continuously and selectively detect biological molecules. In particular, nucleic acid probes show great potential for the rapid identification of human, animal, or plant pathogens,[1,2] in the detection of specific genes in animal and plant breeding,[3] and in the diagnosis of human genetic disorders. Currently, DNA detection techniques use radiochemical, enzymatic, fluorescent, and electrochemiluminescent methods.[4−7] These techniques present some inconvenience due to their need for labeled DNA probes and their separate reaction and detection steps, which preclude *in situ* monitoring.

From a theoretical point of view, biosensors offer a promising alternative based on a very simple principle: a selective biochemical receptor is associated with a transducer, which translates the recognition event into a physically measurable value.[8] This physical parameter depends on the type of transducer used (electrodes, optical fibers, and piezoelectric devices are common) and may be as simple as a variation of the charge or thickness of the transducer-bound receptor layer.

The main problems associated with these devices are the reproducible preparation of the receptor layer and the selection of an adequate transducer, which depends on the type of biological system studied. For instance, amperometric transducers are particularly well-adapted for coupling with redox enzyme systems, because recognition (through enzymatic reaction) provokes consumption or production of redox-active species that are readily detected. The approach is more complicated when dealing with biological binding agents rather than catalysts, since their selective recognition properties are based on affinity, such as the antibody/antigen interaction or the hybridization of a DNA single strand with its complementary strand.

The feasibility of using electrochemical impedance measurements on functionalized heterostructures (semiconductor/dielectric/electrolyte) to directly detect an antibody/antigen interaction by following variations in capacitance,[9] or in-phase impedance,[10] has already been demonstrated. In this study, the possibility of direct, *in situ* detection of hybridization between complementary homo-oligomer DNA strands has been investigated using impedance measurements on functionalized heterostructures.

According to the well-known Watson and Crick model,[11] the DNA molecule consists of two polydeoxynucleotide chains that bind through complementary base pairs (adenine, thymine, cytosine, and guanine) to form a double helical structure. Hybridization of two complementary polydeoxynucleotide strands is a very selective recognition process that involves two steps: the first step is nucleation, which corresponds to contact made between two short complementary regions of DNA, and the second step is the rapid binding of the remaining base pairs forming the strand.[12] In this work, homo-oligomer single strands immobilized onto a Si/SiO_2 substrate play the role of a specific receptor for complementary strands present in solution. Simple synthetic strands of homo-oligomers (refered to as DNA in the following text) have been used to demonstrate the nature of the responses produced by these structures and to illustrate the feasibility of using the field effect for the detection of DNA hybridization.

Experimental Section

Preparation of Samples. The substrates used as electrodes were 1 × 1 cm^2 and 0.3 mm thick, taken from diced Si/SiO_2 wafers (purchased from Microsens, Switzerland). The Si was

* Address correspondence to this author.
[†] Ecole Centrale de Lyon.
[‡] Concordia University.
[⊗] Abstract published in *Advance ACS Abstracts,* March 15, 1997.

S1089-5647(96)03056-8 CCC: $14.00

boron doped to a density of about 10^{15} cm^{-3}. On the back side of the Si/SiO_2 substrate, gold/chromium films deposited under vacuum provided an ohmic contact. The active area of the electrode, where the chemical modifications were performed to produce the sensing layer, corresponds to a circular area of 0.07 cm^2 in the center of the oxide surface. The thickness of the oxide in this central area is close to 100 Å, compared to 1000 Å over the rest of the electrode surface. These electrodes were fabricated to our specifications.

The surface modification was done in four steps: cleaning, functionalization, APTS grafting, and homo-oligomer immobilization. The cleaning procedure consisted of immersing the substrates in boiling methanol for 10 min, rinsing with deionized water, and immersing the substrates in boiling acetone for 10 min, followed by air-drying at room temperature. The generation of OH groups on the silica surface was performed by immersing the substrates in concentrated sulfochromic acid for 3 min and rinsing thoroughly with deionized water. The hydroxylated Si/SiO_2 electrode surface was then coated with 2.5 μL of a 5% aqueous solution of 3-aminopropyltriethoxysilane (APTS, Sigma) and air-dried at room temperature (22 °C) for 1 h. Excess APTS was removed by rinsing the modified electrode with Tris-HCl buffer (10 mM Tris-HCl (Sigma), 50 mM NaCl, pH 7.1) for 20 min. Single-stranded oligos were coupled to the APTS-modified electrode using the *N*-bromosuccinimide method reported by Keller et al.[14] The strands used for immobilization are all synthetic homo-oligomers of either 20 ($(dT)_{20}$) or on the order of a 1000 thymine bases (poly(dT)). A 20 μL sample of an aqueous solution of 0.01 M *N*-bromosuccinimide (Aldrich) was added to 1 mL of a 1 mg/mL solution of single-stranded DNA in 1 M aqueous $NaHCO_3$ and left to react for 15 min at 0 °C. A 2.5 μL sample of *N*-bromosuccinimide/DNA solution was then deposited onto the APTS-derivatized electrode and left to dry at room temperature overnight. The modified electrode was then rinsed with Tris-HCl buffer.

Measurement Procedure. Impedance measurements were performed at frequencies of 20 and 100 kHz, at applied dc potentials ranging from −1 to +1 V vs Ag/AgCl reference electrode, using a classical potentiostatic three-electrode setup (platinum foil counter electrode). The apparatus for measurements at 20 kHz consisted of a potentiostat/galvanostat (Model HA-501G, Hokuto Denko Ltd.) and two lock-in amplifiers (Models SR510 and SR530, Stanford Research Systems), controlled by a PC. For measurements at 100 kHz, a fast three-electrode potentiostat (built at Ecole Centrale de Lyon) was used in conjunction with a single lock-in amplifier (Model SR850, Stanford Research Systems), under PC control. In both cases, a modulated sine signal of weak amplitude (V_{ac} = 10 mV rms, 20 or 100 kHz) taken from the function generator of one of the lock-in amplifiers is fed through the potentiostat and added to the applied dc potential ramp. At 20 kHz, the applied potential, *V*, and the resulting current, *I*, were taken from two separate outputs of the potentiostat/galvanostat, and the signals were measured by two separate lock-in amplifiers (one for *V* and one for *I*). The homemade potentiostat used for experiments at 100 kHz was equipped with an electronic switch controlled by a microcomputer allowing for alternative measurements of the applied potential and the current, using a single lock-in amplifier. The two parameters (*V* and *I*) are measured in-phase and out-of-phase (quadrature) using the sine modulation frequency generated by the lock-in amplifier's internal oscillator as reference. Results are recorded and stored in a PC that calculates the impedance based on the complex form of Ohm's law (see Results and Discussion section).

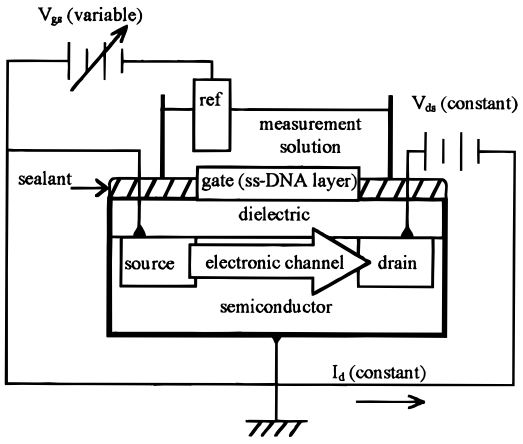

Figure 1. Field effect transistor (FET). Single-stranded DNA (ssDNA) layer is prepared as described in the Experimental Section.

The FETs (field effect transistors), provided by CIME (Grenoble), had a gate area of 20 μm × 500 μm. The electrical setup used for FET measurements is shown in Figure 1. The sealant used to isolate the gate was made by mixing 1.01 g of 825 (Shell) with 0.36 g of Jeffamine D320 (Texaco) and 0.08 g of Aerosil 200 silica (Degussa), which gave enough sealant to cover 10 FETs. After application of the sealant the FETs were left to dry at room temperature for 15 h and the polymerization was then completed by placing them in an oven at 70 °C for 4 h. The measurement is accomplished by imposing a constant potential between the drain and source contacts while maintaining the drain current constant by adjusting the potential between the source contact and the reference electrode. This compensation in potential corresponds to the sensor response, which is read directly in millivolts. The electrolyte used for both impedance and FET measurements was an aqueous solution of 10 mM tris(hydroxymethyl)aminomethane hydrochloride (pH 7.1) and 50 mM NaCl.

The complementary strands used for hybridization were $(dA)_{18}$ and poly(dA) (∼1000 bases). Noncomplementary poly(dC) (∼1000 bases) and calf thymus DNA (type 1) were also used. A 1 mg/mL solution of calf thymus DNA was prepared by dissolving it in 1 M aqueous $NaHCO_3$. Single-stranded calf thymus DNA sequences were obtained by heating the double-stranded DNA solution for 15 min at 90 °C followed by rapid cooling in an ice bath. This provides random sequences (∼15 million bases long) of DNA. All oligo- and polynucleotides used in this study were provided by Sigma.

Two different methods were employed for the hybridization step. *Ex situ* hybridization (batch method) was performed by depositing 2.5 μL of a solution containing either $(dA)_{18}$, poly(dA), or poly(dC) at a concentration of 1 mg/mL in 1 M aqueous $NaHCO_3$ directly onto the modified substrate. The substrate was left to dry at room temperature for 1 h and then thoroughly rinsed with Tris-HCl solution. The cell was then assembled, the electrolyte was added, and the measurement was taken. To follow the evolution of the hybridization process in real time, *in situ* measurements were also performed by adding a certain volume of the complementary DNA solution (1 mg/mL in 1 M aqueous $NaHCO_3$) directly to 10 mL of the buffered electrolyte, mixing thoroughly, and then adding the mixture to the assembled cell. All measurements were done in the dark, to avoid photogeneration of charge carriers in the semiconducting electrode. All measurements were conducted at room temperature (22−25 °C). Denaturation was performed by immersing the electrodes in boiling, deionized water for 0.5 h. Samples not in use were stored in Tris-HCl.

Results and Discussion

Hybridization Detection through Impedance Measurements. The substrate, or transducer, used for these measurements is a semiconductor (silicon) covered with a blocking dielectric layer (a thin silicon dioxide layer), which prevents the occurrence of faradaic phenomena at the interface between the oxide layer and a conducting solution. When used as a working electrode in a classical three-electrode potentiostatic setup, the semiconductor continuously compensates for surface modifications by rearranging its own charge distribution within the space−charge layer. The Si/SiO_2/electrolyte structure is equivalent to that of a metal-oxide-semiconductor (MOS) device and allows detection through the field effect in the semiconductor.

A small-amplitude sine wave (V_{ac}= 10 mV rms, 20−100 kHz) superimposed on the potentiostat's dc potential ramp is applied to the working electrode. Applied potential (V) and current (I) are measured in-phase and out-of-phase (quadrature) with respect to the reference sine wave. The in-phase impedance (Z_p) and out-of-phase impedance (Z_q) can then be calculated using the complex form of Ohm's law:

$$\tilde{V} = \tilde{Z}\tilde{I} = (Z_p + iZ_q)\tilde{I}$$

$$\tilde{V} = V_p + iV_q \quad \text{and} \quad \tilde{I} = I_p + iI_q$$

For each continuous polarization value, and for a given modulation frequency, the in-phase, Z_p, and out-of-phase, Z_q, impedances can be expressed respectively as follows:

$$Z_p = \frac{V_pI_p + V_qI_q}{I_p^2 + I_q^2} \quad \text{and} \quad Z_q = \frac{V_qI_p - V_pI_q}{I_p^2 + I_q^2}$$

The general shapes of the $Z_p(V)$ and $Z_q(V)$ curves obtained at frequencies of 20 and 100 kHz are shown in Figure 2a,b, respectively. The $Z_q(V)$ curves illustrate the three characteristic regimes of the underlying p-type semiconductor, as a function of the applied potential: (i) the accumulation regime for positive potential V vs Ag/AgCl electrode; (ii) the inversion regime for negative V; and (iii) the strong decrease in Z_q values at intermediate potentials corresponding to the depletion regime. These curves can be analyzed in terms of an equivalent electrical scheme, which demonstrates that the peak in the $Z_p(V)$ curve, for example, corresponds to the surface states at the Si/SiO_2 interface. The position and the amplitude of the maximum relate respectively to the energy and the density of the surface states. On the basis of this analysis, it has also been shown[13] that it is preferable to perform these measurements in the high-frequency range (20−100 kHz) in order to diminish the conductive contribution of the surface states (trapping and recombination processes) and better isolate the capacitive effects. In the depletion regime, the semiconductor is very sensitive to all events occurring at the surface of the heterostructure. Under thermodynamic equilibrium conditions, adjustment between the semiconductor Fermi level and the equivalent energy level in solution (defined as the solution's redox potential) induces a charge distribution within the space charge layer of the semiconductor to maintain electrical neutrality. This is represented by band bending within the semiconductor. The flat-band potential, V_{fb}, is defined as the potential that must be applied to the device (vs a reference electrode in solution) to cancel this band bending, and the value of V_{fb} is determined by extrapolating the slope of the $Z_q(V)$ curve in the depletion regime to the applied potential axis. If the charge at the oxide/electrolyte interface is modified, the underlying semiconductor

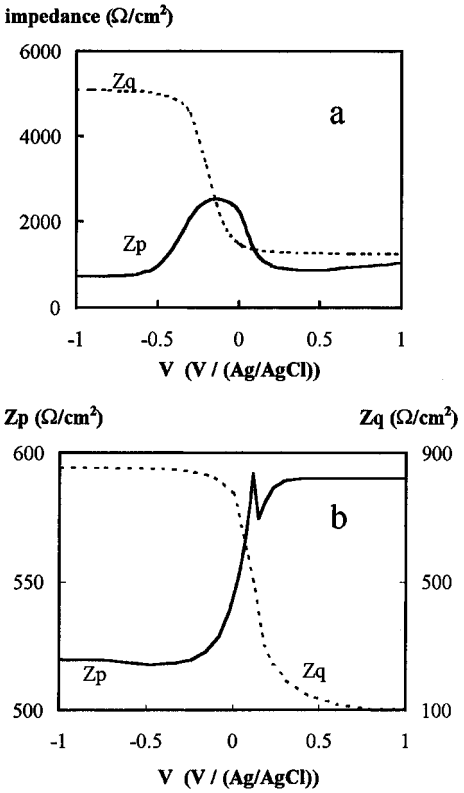

Figure 2. Typical shape of electrochemical in-phase (Z_p) and out-of-phase (Z_q) impedance curves as a function of applied potential, obtained with the semiconductor/dielectric/electrolyte structure: (a) 20 kHz and (b) 100 kHz.

compensates for this modification by a new charge distribution inside its space charge layer to maintain electrical equilibrium. This induces a change in the band bending and therefore yields a new value for the flat-band potential, which is reflected by a displacement of the impedance curves along the potential axis.

Figure 3 shows Z_q vs applied potential obtained with a sample electrode under similar experimental conditions (frequency of 100 kHz), after single-stranded DNA immobilization (curve 1), and after *ex situ* hybridization with complementary poly(dA) (curve 2). A curve shift toward negative potentials is systematically obtained after the *ex situ* hybridization step. Curve 3 in Figure 3 shows that this shift is reversed after the denaturation process. Successive hybridization and denaturation steps performed with the same electrode give reproducible shifts of the Z_q curves along the potential axis, corresponding to an average shift of the flat-band potential, V_{fb}, of 100 mV (for three consecutive hybridization−denaturation steps). Similar shifts are observed when using $(dA)_{18}$. By contrast, no shifts are observed when electrodes with immobilized $(dT)_{20}$ are exposed to a solution containing noncomplementary poly(dC), at the same concentration (Figure 4).

Figure 5 shows the time evolution of the $Z_q(V)$ curves during an *in situ* hybridization run, following the addition of 20 μL of poly(dA) solution to 10 mL of the buffered cell electrolyte. The overall shift in flat-band potential is again of about 100 mV. By plotting the variation of Z_q with time, at a fixed potential of −0.3 V vs Ag/AgCl in the depletion regime (from Figure 5), the shift is seen to be relatively rapid within the first 3 h, and the process is essentially completed after 4 h (Figure 6). The time course of the signal is comparable to that obtained by Su et al., where an acoustic network analysis was used to study the kinetics of cDNA hybridization at the surface of piezoelectric electrodes modified with ss pPT-2DNA.[15] A similar hybridization rate was also obtained by Millan et al.[16] with a voltammetric

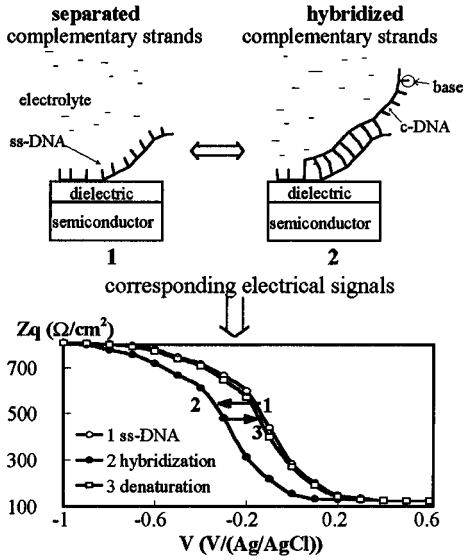

Figure 3. Electrical effects induced by hybridization between complementary strands. Curve 1 was recorded after immobilization of ssDNA onto the substrate, which acts as a receptor for the specific recognition of complementary strands. Curve 2 corresponds to the impedance measurements after hybridization. Curve 3 shows the impedance measurements after denaturation, where the double strands are separated and a reversible shift of the impedance curve is observed (measurements performed at a frequency of 100 kHz).

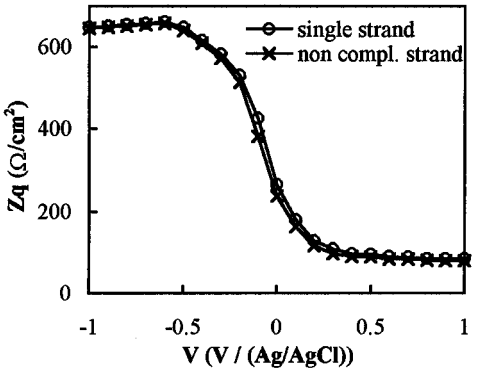

Figure 4. Interaction of a substrate with immobilized $(dT)_{20}$ in contact with noncomplementary poly(dC) (frequency of 100 kHz). No significant shift occurs.

DNA biosensor, using immobilized poly(dT) and 10 μg/mL of soluble poly(dA) in 5 mM Tris (pH 7.0) with 20 mM NaCl. This study showed that faster (10 min) hybridization can be achieved in 0.5 M NaCl, as is the case for hybridization in solution.[17]

To identify possible interference effects during hybridization of complementary strands, *in situ* measurements were also done in the presence of single-stranded calf thymus DNA. Addition of 20 μL of calf thymus DNA solution to 10 mL of electrolyte solution causes no shift of the flat-band potential during a period of 24 h, as illustrated in Figure 7. *In situ* hybridization of 20 μL of a 1:1 mixture of single-stranded calf thymus DNA and $(dA)_{18}$ or poly(dA) with both types of modified electrodes ($(dT)_{20}$, poly(dT)) were compared. Flat-band potential shifts similar to those obtained with pure synthetic single strands were observed. Figure 8 shows the result obtained when poly(dA) is hybridized with poly(dT) in the presence of calf thymus DNA.

It should be noted that the 1:1 ratio is a mass ratio, and therefore the number of calf thymus DNA sequences present in the electrolyte is lower than that of the synthetic strands used, by approximatively 4 orders of magnitude. However, the overall number of bases associated with each type of strand present is

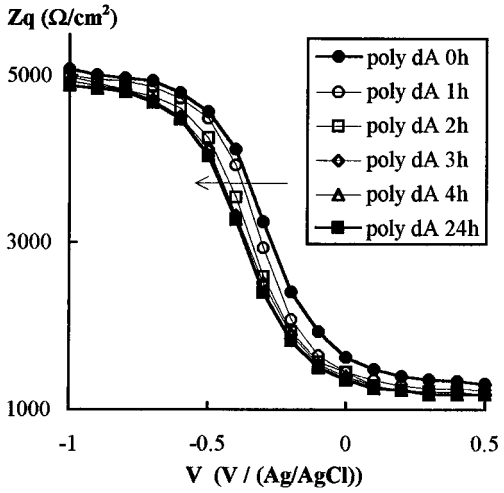

Figure 5. Time evolution of the $Z_q(V)$ curves during *in situ* hybridization with complementary poly(dA) (frequency of 20 kHz).

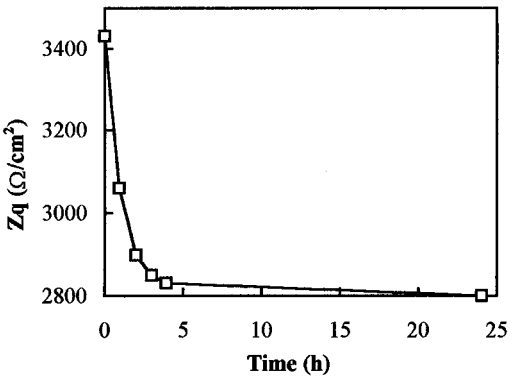

Figure 6. Variation of Z_q with time, taken at an applied dc potential of −0.3 V vs Ag/AgCl (from Figure 5).

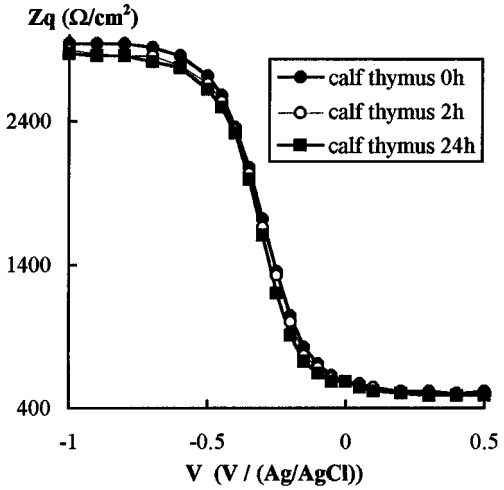

Figure 7. Out-of-phase impedance measurements of a poly(dT)-modified electrode, *in situ* hybridized with single-stranded calf thymus DNA (20 kHz).

equivalent. The calf thymus DNA offers a multitude of sites where hybridization with the synthetic homo-oligo- and polynucleotides could occur, and interference effects might be expected. Under these conditions no such effects were observed.

On the basis of the results presented, we can conclude that the changes seen in flat-band potential are actually due to a specific and reversible interaction between immobilized single-stranded DNA and its complementary strand. The hybridization process affects the distribution of surface charge and provokes a field effect across the heterostructure.

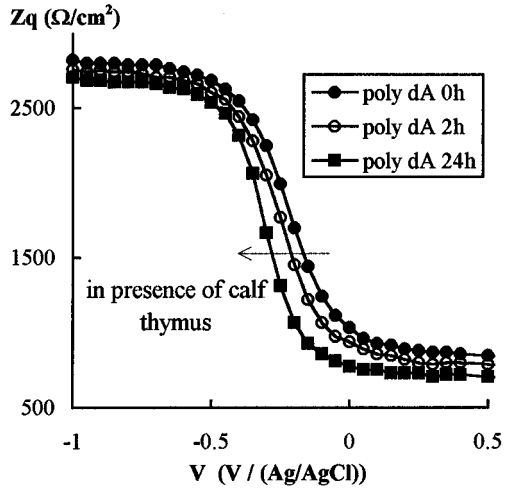

Figure 8. Out-of-phase impedance measurements of a poly(dT)-modified electrode, *in situ* hybridized with a 1:1 solution of poly (dA) and single-stranded calf thymus DNA (20 kHz).

Surface Charge and Flat-Band Potential Shift. The variation of charge, Q_s, at the oxide/electrolyte interface produces, by field effect, a reorganization of the charge in the near surface region of the semiconductor/oxide interface, i.e. a variation of the surface potential ψ_s, and consequently a variation of the flat-band potential V_{fb}. The variation of V_{fb} is directly related to the variation of ψ_s. The following theoretical treatment illustrates the relationship between Q_s, ψ_s, and V_{fb} for the specific semiconductor/dielectric/electrolyte (SDE) structure used in these studies.[18]

The SDE structure is considered as being ideal with no Si/SiO_2 interface states and no space charges in the oxide. We also assume that when the amount of charge Q_s varies at the oxide/electrolyte interface, due to hybridization, an equivalent variation of charge of opposite sign is induced in the semiconductor at the Si/SiO_2 interface. The problem is then reduced to calculating the relationship between Q_s and ψ_s within the semiconductor at the Si/SiO_2 interface.

The starting point of the calculation is Poisson's equation, which relates the potential ψ to the charge distribution ρ, in the semiconductor at a given distance x from the interface.[18] This takes into account the majority and minority charge carriers as well as the density of donor states.

$$\frac{\partial^2\psi}{\partial x^2} = -\frac{\rho(x)}{\epsilon_s}$$

Integration of this equation over x gives the electric field as a function of distance from the interface, which yields a value E_s for the electric field at the Si/SiO_2 interface. The amount of charge necessary to produce this field is $Q_s = \epsilon_s E_s$, where ϵ_s is the permitivity of the semiconductor. Finally, we obtain

$$Q_s = \mp\frac{2\epsilon_s kT}{qL_D}\left[(e^{-\beta\psi} + \beta\psi - 1) + \frac{n_0}{p_0}(e^{\beta\psi} - \beta\psi - 1)\right]^{1/2}$$

$$\beta = \frac{q}{kT} \quad \text{and} \quad L_D = \sqrt{\frac{2\epsilon_s}{qp_0\beta}}, \quad \text{sign} + (-) \text{ for } \psi > 0\ (< 0)$$

where L_D is the extrinsic Debye length, n_0 and p_0 are the equilibrium minority and majority charge carrier densities taken at $T = 300$ K, respectively, q is the elementary charge, and k is the Boltzmann constant. Using values of 10^{15} cm^{-3} for the doping density, which yields $n_0/p_0 = 4 \times 10^{-10}$, and $\epsilon_s = 1.03 \times 10^{-12}$ F cm^{-1}, the plot shown in Figure 9 is obtained for Q_s vs V_{fb}.

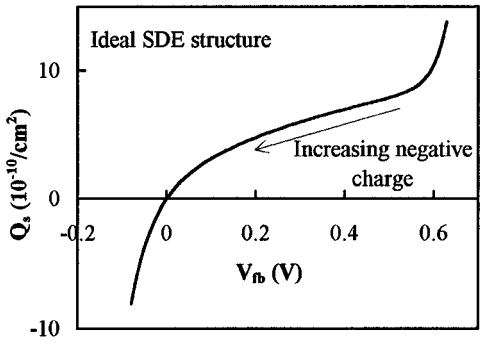

Figure 9. Relationship between surface charge (Q_s) and flat-band potential (V_{fb}) for the ideal SDE structure.

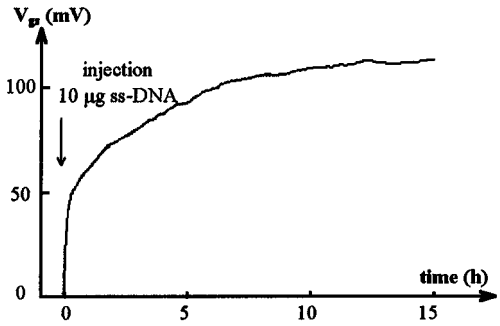

Figure 10. Response of the FET to *in situ* hybridization between $(dT)_{20}$ and poly(dA).

The plot shows that a negative shift of the flat-band potential is expected for an increase in negative charge at the oxide/electrolyte interface. This is observed for the experiments presented here, which would indicate that the effect of the hybridization process is to increase the overall negative charge present at the modified SiO_2 surface. It should be noted that since an ideal SDE structure was considered in these calculations, the Q_s vs V_{fb} curve gives only relative information in terms of the direction of the V_{fb} shift as a consequence of whether the SiO_2 surface becomes more positively or more negatively charged. A more detailed quantitative analysis would require considering the presence of interface states and the space charge of the oxide.

Direct Measurements of Flat-Band Potential Shifts Using FETs. These impedance measurements can be extended to a field effect device where the selective DNA layer serves as a substitute for what is usually a metallic grid. $(dT)_{20}$ was immobilized as previously described. The field effect transistor used in the constant current mode essentially provides access to the same information one obtains from the impedance measurements, shifts in flat-band potential. The advantage of the FET, however, is that it enables direct observation of these shifts, which should correlate in magnitude with those determined by impedance measurements. For the FET-based measurements, it is important to ensure that only the DNA-modified oxide layer is in contact with the solution, and therefore, a perfect encapsulation is required to avoid short-circuiting the device.

Figure 10 shows the response of a modified FET observed under *in situ* hybridization conditions similar to those used for the impedance measurements illustrated in Figure 5. The FET was first put in contact with 5 mL of Tris-HCl buffer electrolyte, and a base line was recorded. The FET was then placed in contact with 5 mL of solution containing complementary strands

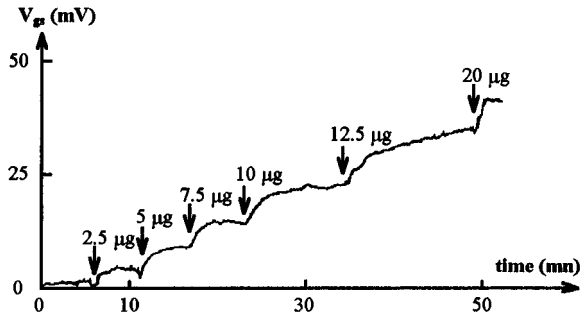

Figure 11. Sensitivity of the FET to the successive introduction of poly(dA). The total quantity of poly(dA) in the solution is indicated.

(prepared by adding 10 μL of a 1 mg/mL in 1 M aqueous $NaHCO_3$ solution of poly(dA) to 5 mL of the Tris electrolyte, and mixing). The signal increases rapidly, and a maximum amplitude of 120 mV is reached after 15 h; 50% of the total response is obtained within 1 h and 90% after 4 h. This response is in good agreement with the impedance measurements, which also exhibited a similar time course and a shift of about 100 mV.

Figure 11 shows the evolution of the signal in response to successive additions of poly(dA). In this case, microliter amounts of the 1 mg/mL in 1 M aqueous $NaHCO_3$ solution of poly(dA) were added directly to the Tris-HCl electrolyte with a micropipet, by placing the tip in close proximity to the modified FET surface. The electrolyte/DNA solution was not stirred during these additions. Although the signals are seen to equilibrate more rapidly and to have weaker amplitudes compared to the results shown in Figures 6 and 10, they show a consistent and direct dependence on the quantity of poly(dA) added.

Conclusion

Using a semiconductor/dielectric/electrolyte structure, we have observed through impedance measurements that hybridization of surface-immobilized synthetic homo-oligomer DNA strands with the complementary strands in solution provokes a significant shift of the impedance curves along the potential axis. This shift corresponds to a change in the flat-band potential of the underlying semiconductor in response to the modification of surface charge induced by recognition and hybridization between the complementary homo-oligomer strands. This result has been exploited in a device able to detect a particular homo-oligomer DNA sequence directly, *in situ* and without labeled species. The sensor is based on a field effect transducer and a recognition layer composed of homo-oligomer strands. Selectivity, sensitivity, and reversibility of the sensor have been demonstrated. These results show the promise of such devices for applications in medical diagnostics and molecular biology. Future work will be aimed at optimizing the device, and the use of oligomer sequences of greater complexity will also be investigated. The sensor represents a simple, inexpensive approach to the direct and *in situ* detection of natural DNA sequences.

Acknowledgment. The authors are grateful for financial support from the Centre National de la Recherche Scientifique (France), the Centre Jacques-Cartier, and the National Sciences and Engineering Research Concil of Canada. Support for I.L. through a "Bourse d'Excellence" postdoctoral fellowship from the Quebec Ministry of Education is gratefully acknowledged. Support for J.P.C. through an International Fellowship, Department of External Affairs and International Trade of Canada, is also gratefully acknowledged.

References and Notes

(1) Wachsmuth, K. *Infect. Control* **1985**, *6*, 100.
(2) Caskey, T. *Science* **1987**, *236*, 1223.
(3) Hillel, J.; Schaap, T.; Haberfeld, A.; Jeffreys, A. J.; Plotzky, Y.; Cahaner, A.; Lavi, U. *Genetics* **1990**, *124*, 783.
(4) Sutherland, G.; Mulley, J. In *Nucleic Acid Probes*; Symons, R. H., Ed.; CRC Press: Florida, 1989; pp 159−201.
(5) Kricka, L. J. *Nonisotopic DNA Probe Techniques*; Academic Press: Toronto, 1992; pp 3−19.
(6) Keller, G. H.; Manak, M. M. *DNA Probes*; Macmillan (Stockton Press): New York, 1989; pp 149−213.
(7) Dicesare, J.; Grossman, B.; Katz, E.; Picozza, E.; Ragusa, R.; Woudenberg, T. *BioTechniques* **1993**, *15*, 152.
(8) Downs, M. E. A. *Biochem. Soc. Trans.* **1991**, *19*, 39.
(9) Bataillard, P.; Gardies, F.; Jaffrezic-Renault, N.; Martelet, C.; Colin, B.; Mandrand, B. *Anal. Chim. Acta* **1988**, *60*, 2374.
(10) Souteyrand, E.; Martin, J. R.; Martelet, C. *Sens. Actuators*, B **1994**, *20*, 63.
(11) Watson, J. D.; Crick, F. H. C. *Nature* **1953**, *171*, 738.
(12) Zubay, G. *Biochemistry*; Macmillan Publishing: New York, 1988; pp 211−256.
(13) Nicollian, E. H.; Brews, B. *MOS Physics and Technology*; Wiley: New York, 1982.
(14) Keller, G.; Cummina, C.; Haung, D.; Monak, M.; Ting, R. *Anal. Biochem.* **1988**, *170*, 441.
(15) Su, H.; Kallury, K. M. R.; Thompson, M.; Roach, A. *Anal. Chem.* **1994**, *66*, 769.
(16) Millan, K. M.; Saraullo, A.; Mikkelsen, S. R. *Anal. Chem.* **1994**, *66*, 2943.
(17) Meinkoth, J.; Wahl, G. *Anal. Biochem.* **1984**, *138*, 267.
(18) Sze, S. M. *Physics of Semiconductor Devices*; Wiley-Interscience: New York, 1969; pp 28, 425−504.